Confocal Scanning Laser Microscopy of Polymer Coatings

X. LING, M. D. PRITZKER, J. J. BYERLEY, C. M. BURNS

Department of Chemical Engineering, University of Waterloo, Waterloo, Ontario N2L 3G1, Canada

Received 3 April 1997; accepted 26 May 1997

ABSTRACT: A new nondestructive technique, confocal scanning laser microscopy (CSLM), is described that is used to characterize the topography and morphology of polymer coatings. The topography of the coating can be determined even when the coating is completely opaque. When the coating is not completely opaque, CSLM has the distinct advantage of also being able to distinguish between the coating surface and the substrate, thus enabling coating thickness to be determined over a wide range of areas. In this study CSLM was successfully applied to poly(2-vinylpyridine) coatings formed on mild steel substrates by *in situ* electropolymerization. Satisfactory morphological details were obtained for areas ranging from 200 × 200 μm to 4 × 4 mm. Quantitative measurements of the coating thickness and the surface roughness distribution were also carried out. Although several other nondestructive techniques for coating morphological analyses are available, CSLM has unique advantages in being able to provide simultaneous qualitative and quantitative information on coating surfaces as well as measurements over a wide range of surface areas. A comparison of CSLM with other popularly used methods is provided and the characteristics and limitations of the various techniques are discussed. © 1998 John Wiley & Sons, Inc. J Appl Polym Sci **67:** 149–158, 1998

Key words: confocal scanning laser microscopy; topography; morphology; electropolymerization; poly(2-vinylpyridine); coating

INTRODUCTION

Morphological analysis is one of the important factors in evaluating the quality of polymer coatings, especially the uniformity and thickness that greatly influence the coating performance properties. Minute flaws (i.e., pits and cracks) in the coatings will also affect coating properties such as conductivity, permeability, and corrosion resistance. Thus, it is useful to have a clear evaluation of the morphological characteristics of the formed polymer coating. A convenient and reliable method for nondestructive analysis, which can provide a detailed evaluation of the morphology of the coating such as its roughness and thickness, is essential in selecting the most suitable synthesis technique for producing the coatings.

Quantitative measurement of the thickness of the coating and qualitative observations of the morphology of the coating have conventionally been carried out by separate techniques. The former is usually accomplished by estimating the weight increase of a coated sample (gravimetry), while the latter is commonly done by scanning electron microscopy (SEM) or scanning tunneling microscopy (STM). Other techniques such as magnetic induction, eddy current, radioisotope backscattering, resistivity measurement, and X-ray fluorescence have also been applied occasionally for evaluating polymer coatings. Due to the complexity of the coating properties (e.g., conductivity, uniformity, fluorescence, and other optical and thermal properties) and the limitations of these various techniques, however, the application of these techniques is often limited. For ex-

Correspondence to: Prof. C. M. Burns.

Journal of Applied Polymer Science, Vol. 67, 149–158 (1998)
 CCC 0021-8995/98/010149-10

ample, the magnetic induction method can only be used for steel substrates; the eddy current technique requires that the substrate and the coating have sufficiently different electrical conductivities; the radioisotope backscattering technique requires the atomic numbers of the coating and substrate materials to be significantly different; the X-ray fluorescence technique has the severe constraint that many synthesized polymers contain fluorescein; and the resistivity measurement method can be applied only to insulating coatings and can be influenced by many factors concurrently (e.g., coating composition and uniformity, the presence of coating defects, adhesion between the coating and the substrate, and variations in the geometry of the substrate and in the preparation of the surface). An independent calibration curve is often needed for each individual case. A number of recent publications describing the application of these methods for evaluating coating morphology are available in the literature.[1–12] A brief assessment of the more popular techniques is given in the next section.

In this work we applied confocal scanning laser microscopy (CSLM) as a new nondestructive method to analyze the topography and morphology of a polymer coating. The technique is fast and easy to operate. It can provide high resolution images of the surface and quantitative measurement of the surface roughness and the coating thickness. Although our application is on poly(2-vinylpyridine) coatings formed on mild steel substrates by *in situ* electropolymerization,[13] the technique can be applied to a wide range of coating–substrate systems. The principles and history of the development of CSLM are presented as well as a detailed description of its application to poly(2-vinylpyridine) coatings formed by electropolymerization.

CURRENT TECHNIQUES FOR MORPHOLOGICAL ANALYSIS

There are a number of techniques for investigating the morphology of surfaces. As mentioned previously, however, the techniques for surface profile evaluation and for quantitative coating thickness and roughness measurements are often separated. Gravimetry is the most widely used technique for the measurement of coating thickness; SEM and STM are the most popularly used methods for the observation of surface morphology.

Gravimetry

Gravimetry involves determining the mass change of a sample as a result of coating formation. In the case of coatings formed electrochemically, it is usually done either by directly recording the sample weight changes before and after coating formation[14–18] or by measuring the total amount of charge passed in the process and calculating the coating mass using basic electrochemical relations such as Faraday's Law.[19–23] When only a thin polymer coating on a metal substrate is formed, the coating weight is normally very small compared to the weight of the metal substrate, which can lead to a significant relative error in the estimate of the coating weight. A major problem with the second approach stems from the fact that only the initiation step during electropolymerization involves electron transfer, whereas the propagation and termination steps do not.[24] In addition, it is acknowledged that some side electrochemical reactions (e.g., hydrogen evolution[13] and metal substrate oxidation[25]) usually accompany the electropolymerization, making charge transfer more difficult to interpret. The determination of the coating thickness from the coating weight is also subject to error because it is necessary to have an accurate value of the actual coating density,[22,26,27] which may not be available.

SEM

Although SEM[28] has been widely used to examine polymer coatings,[18,20,23,29–31] it has several disadvantages. Frequently, organic coatings must be coated with gold or other conductive materials.[15,32,33] Experimental conditions, such as high vacuum and beam heating, may alter or damage the coating surface. Furthermore, quantitative data, such as coating thickness and surface roughness distribution, cannot be obtained by SEM.

STM

The principles and the applications of STM have been described in some recent publications.[34–38] STM has found increasing use for both metal and polymer thin films.[39–42] Because the tunneling current is very sensitive to the distance between the substrate and the probe, STM is not well suited for large areas or rough surfaces.

CSLM

CSLM offers the distinct advantage of eliminating defocused images rather than creating a blur of

those images as in standard microscopy. The intensity of the CSLM image drops sharply as the image is defocused, whereas the intensity does not change with a standard microscope. Thus, the plane that is in focus can be observed without interference from layers above or below. This property allows imaging of structures with height differences comparable to the wavelength of the laser beam, thus permitting quantitative measurements of surface roughness. Its defocusing characteristic also permits optical cross sectioning of a nonopaque specimen and can distinguish between coating and substrate. This allows the quantitative measurement of coating thickness. CSLM images tend to have sharper edges and stronger contrast than images obtained with a standard microscope. It is convenient to operate, it can perform scans rapidly, and it does not damage the specimen. There are no strict requirements on the coating and substrate materials in order for CSLM to image the surface topography. Measurement of coating thickness, however, does require that the coating not be completely opaque.

The principle of confocal microscopy was first described by Young and Roberts.[43] The details of this type of imaging were first described by Minsky.[44] Davidovits and Egger[45] were the first to develop a working laser-based confocal microscope. Wilson and Sheppard[46] and Wilson[47] provided a detailed analysis of this technique. Dixon et al.[48] developed a transmitted-light and reflected-light scanning stage microscope, which uses the same confocal detector for both reflected and transmitted light. The transmitted beam is reinjected into the optical path of the microscope parallel to the reflected beam. The microscope forms images both in transmission through the top and bottom of the specimen as well as in reflection from the top and bottom of the specimen. The various beams are separated by placing a half-wave plate and a polarizer in the transmission arm of the microscope and a second polarizer in the detection arm of the microscope. This has the advantage of imaging large area samples with very high resolution. Recently, the first practical scanning beam confocal transmission microscope was described, along with new applications in transmission.[49] This device has all the advantages of a scanning stage microscope in addition to producing a high resolution image (512×512 pixels and 256 grey levels) in less than 2 s. Because the contrast mechanisms for these images are different, the reflection and transmission images contain complementary information. The optical slicing property of the confocal microscope is used to obtain single confocal slice images in transmission and reflection. The modified confocal scanning beam laser microscope developed by Dixon et al.[48] was used in our study to analyze polymer coated surfaces.

It should be emphasized that the use of CSLM for quantitatively analyzing the morphology of coatings is a recent development. Only recently it was used to measure surface roughness of copper deposits produced electrolytically.[50] However, because this deposit was opaque, its thickness could not be determined. The present work involves morphological analysis of poly(2-vinylpyridine) coatings on mild steel substrates formed by *in situ* electropolymerization. The polymer coatings have the additional advantage of not being completely opaque, which allows their thickness to be determined. We believe that the results reported in this article represent the first use of CSLM for this purpose. Before discussing the images obtained using CSLM, a brief description of the electropolymerization process is given in the next section.

PREPARATION OF COATINGS BY ELECTROPOLYMERIZATION

Details of the electrochemical process and the proposed mechanism have been described elsewhere.[13] A three-electrode system was used for the electropolymerization. The working electrodes were SAE 1018-1020 mild steel coupons (C, 0.20 wt %; Mn, 0.60 wt %; P, 0.04 wt % maximum; S, 0.05 wt % maximum) with active surface areas of 5.5 cm^2. The counterelectrode was a platinum wire and the reference electrode was a saturated calomel electrode (SCE, Aldrich Chemical Company). The working electrode was cleaned ultrasonically in a soap solution for 30 min and then polished carefully with SiC-type abrasive paper (up to 1200 grade). Degreasing was carried out with trichloroethylene (TCE) for 2 min, followed by a washing with soap solution to remove the grease and TCE, a rinsing with a large amount of deionized water, and finally a rinsing with ultrapure water (Millipore® ultrapure water system). The prepared metal samples were stored in a desiccator over calcium hydroxide until needed. Because the 2-vinylpyridine monomer (Aldrich Chemical Company) was inhibited with 0.1 wt % of *p-tert*-butylcatechol as received, it was necessary to purify the monomer before use. Purification was carried out by distilling the monomer at

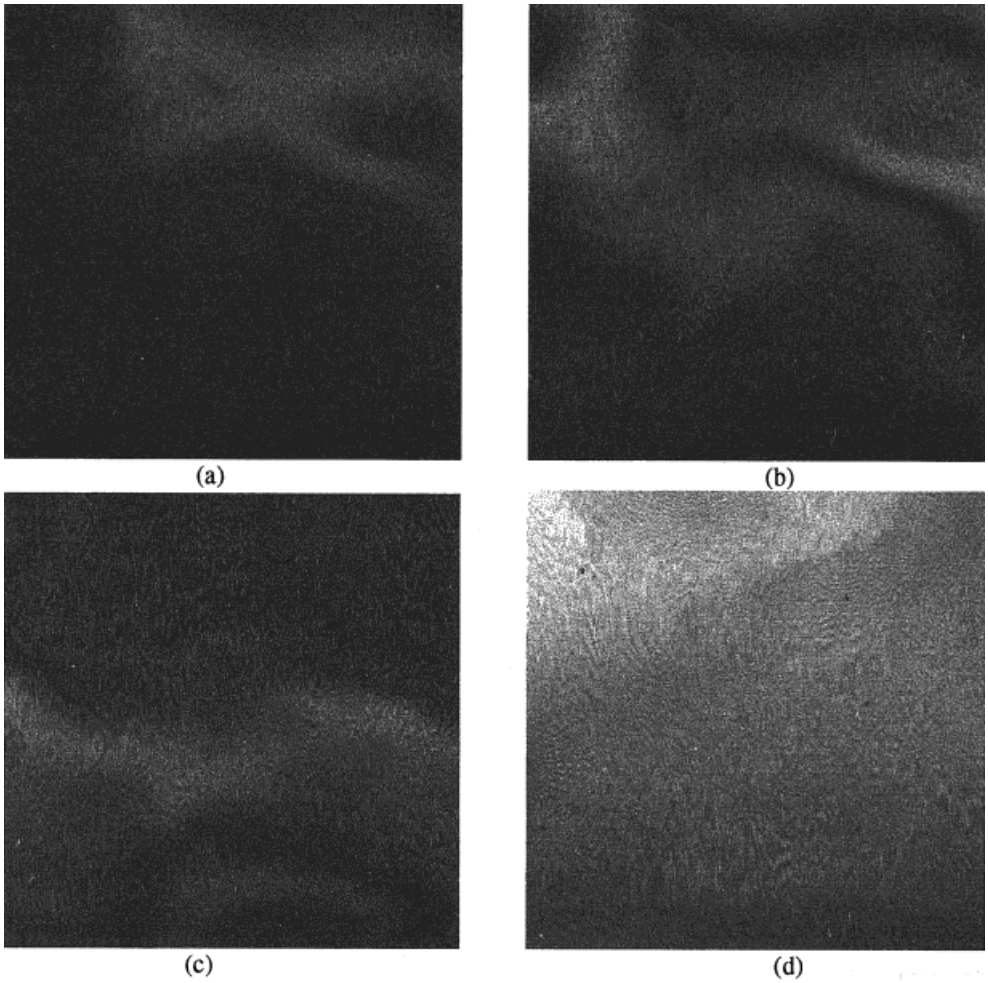

Figure 1 CSLM images of a poly(2-vinylpyridine) coating formed by electropolymerization (200 × 200 μm). (a)–(c) Single images from the beginning, the middle, and the end of the entire image set. (d) The complete surface image from the entire image set.

70°C under vacuum (30 in. Hg). All other chemicals were analytical grade and were used without further purification. The solvent was a water–methanol mixture (volume ratio of 8 : 2); NH_4ClO_4 was used as the supporting electrolyte (0.05*N*) and $HClO_4$ was used to adjust the solution pH to 4.85. All solutions were prepared with ultrapure water and a total volume of 60 mL solution was used in each experiment.

Experiments were performed at 20°C and 1 atm. A potentiostat (EG&G 273) was used to control the electrochemical reaction. Cyclic potential sweep electrolysis in which the electrode potential was varied at a scan rate of 30 mV/s over a range from −0.7 to −2.5 V (vs. SCE) was used to produce the coatings. The solution was agitated using a magnetic stir bar throughout the electrolysis. The current response from the experiments was recorded on a data logging computer (JPC 386SX) and was also monitored on-line on a computer screen. After electrolysis, the coated samples were rinsed with deionized water and dried in a vacuum for 1 day. Characteristics of the polymer coating were examined by U.V.-visible spectroscopy (Beckman Spectrophotometer DU 600) in a wavelength range of 190–1100 nm. The weight change of the samples before and after electropolymerization was recorded as an approximate method to determine coating thickness measurement in order to compare with the results from the CSLM analysis.

The coatings formed had a greenish-brown color, and the electrical resistance was found to be infinite. The coatings were slightly soluble in

methanol and the U.V.-visible spectra showed a characteristic peak at 263 nm, which confirmed the formation of poly(2-vinylpyridine).[51] As noted by previous researchers,[23] it was difficult to measure the average molecular weight of the formed polymer because the polymer coating had a very low solubility in common solvents used for gel permeation chromatography [e.g., tetrahydrofuran (THF), trichlorobenzene (TCB), and TCE]. This fact suggests that the poly(2-vinylpyridine) formed by electropolymerization was at least partially crosslinked.

IMAGE PROCESSING AND ANALYSIS

A model-1135P UNIPHASE® He-Ne laser (1 mW, wavelength of 632.8 nm) was employed as the illumination for surface scanning. The optical diagram, experimental apparatus, and detailed operating parameters have been published elsewhere.[48,49] The image processing procedure of the CSLM is presented by showing and discussing the images of the poly(2-vinylpyridine) coatings. The images shown in Figure 1 represent a 200 × 200 μm area of a coating of poly(2-vinylpyridine) obtained after a 2-h cyclic potential sweep electrolysis. The images represent the end product of the entire process of the CSLM scanning operation, which is continually observed on a monitor. The process involves first focusing the laser beam just above the coating surface so that no distinct image of any part of the surface appears on the monitor. Then the focus of the laser beam approaches the surface gradually and the locations of the elevated points on the surface are observed. Eventually the laser beam passes through the entire surface slice by slice and becomes focused within the bulk of the coating so that all the distinctive images disappear from the monitor. A series of surface intensity images are taken throughout this scanning process. This procedure is performed automatically by an on-line computer system. The number of images taken and the depth over which the laser beam is focused are predetermined and set according to the roughness and thickness of the coating. Figure 1(a–c) is three slice (intensity) images taken from the entire set of images, located at the beginning, middle, and end of the entire image set, respectively. As indicated above, only focused parts of the surface are clearly shown in each image, while all other parts of the surface are out of focus and appear black or blurred. By combining the entire set of intensity images, a map of the maximum intensities across the whole surface is obtained [Fig. 1(d)]. It is important to note that this combined image does not give a true representation of the surface roughness because the maximum intensities at different locations will not likely occur in the same plane. As described below, further processing of the images enables quantitative measure of roughness to be obtained.

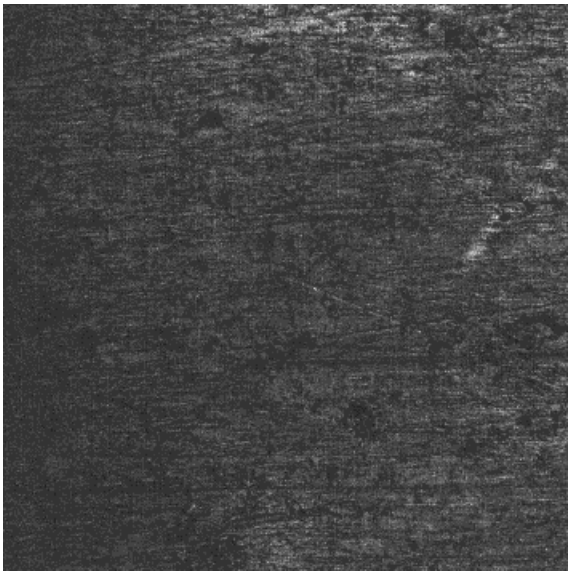

Figure 2 A CSLM image of the metal substrate underneath the coating in Figure 1.

Because the poly(2-vinylpyridine) coating is not completely opaque, the laser beam can penetrate the entire coating and focus on the surface of the steel substrate. Following the same procedure as discussed above, a maximum intensity image of the steel substrate can be obtained without interference from the above coating layer. The relevant image is shown in Figure 2. From these maximum intensity images and their corresponding depths, it is relatively easy to obtain surface depth profiles and to reconstruct 3-dimensional (3-D) topographic images of the scanned surfaces. The 3-D reconstructed surface topographic images of the coating and substrate in Figures 1 and 2 are presented in Figure 3(a,b), respectively, with the coating depth magnified compared to the width of the scanning area. These 3-D reconstructed images have the advantage of providing a better stereoscopic expression of the concerned surfaces. Comparing these two figures shows that the topography of the polymer coating conforms to the topography of the metal substrate reasonably well, although it is somewhat smoother. It should

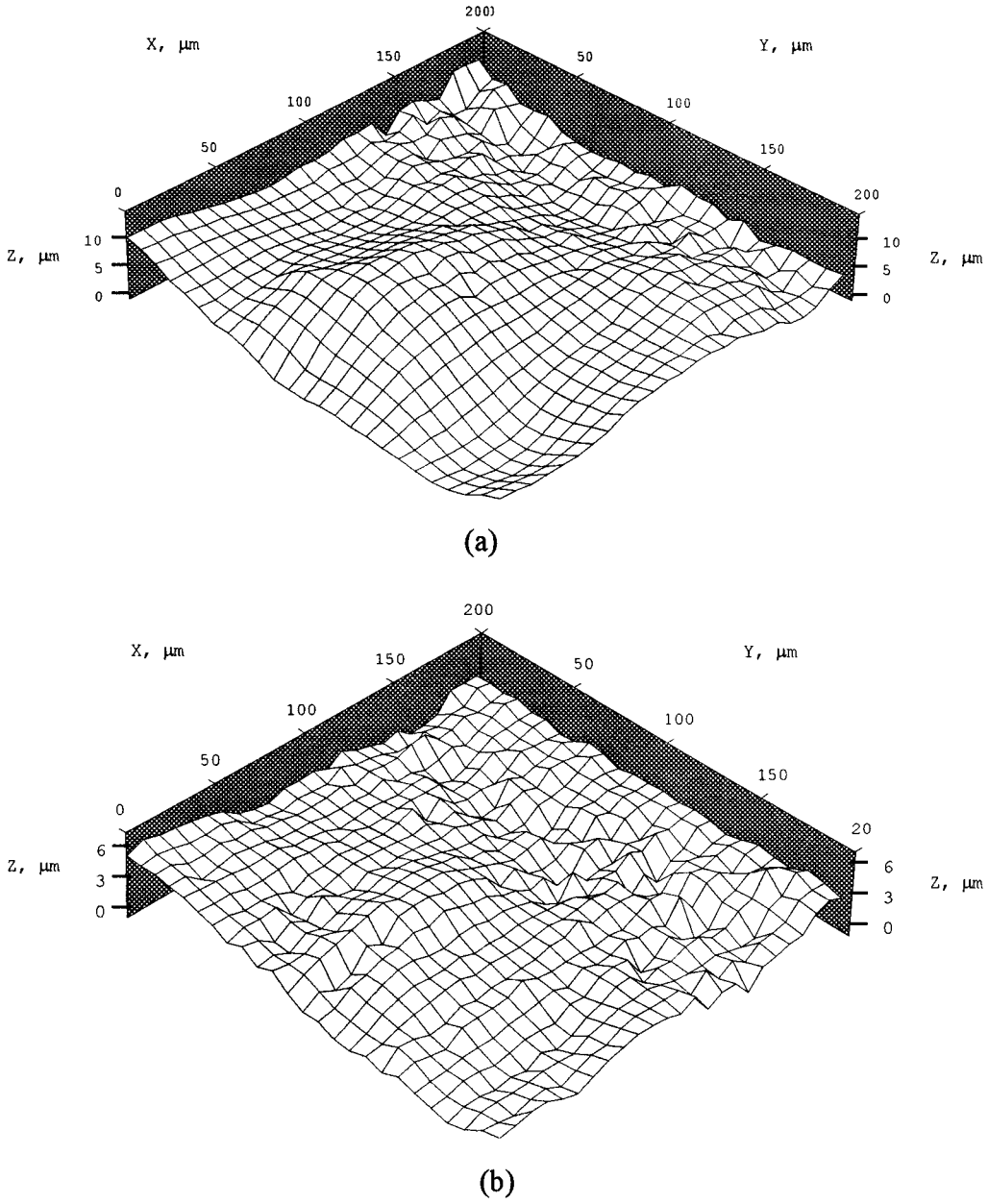

Figure 3 3-D reconstructed surface topography of (a) the polymer coating and (b) the metal substrate in Figures 1 and 2.

be noted that the coatings being analyzed are smooth and so the images do not have many distinct features.

Because the reflected light only has high intensity at the air–coating and coating–substrate interfaces and essentially zero intensity within the bulk of the air, coating, and substrate, a profile of the coating thickness along a line can be obtained by performing a cross-sectioning scan of the laser beam over the line. An on-edge profile of the coating thickness over a randomly selected direction at the same location shown in Figure 1 and Figure 2 is given in Figure 4(a). The two bright bands highlight the top outlines of the polymer coating and the metal substrate. This method gives direct visualization of the thickness and uniformity of the coating. The coating thickness at any given point or the average value over a particular distance can be determined by measuring the light intensity as a function of depth into the sample at

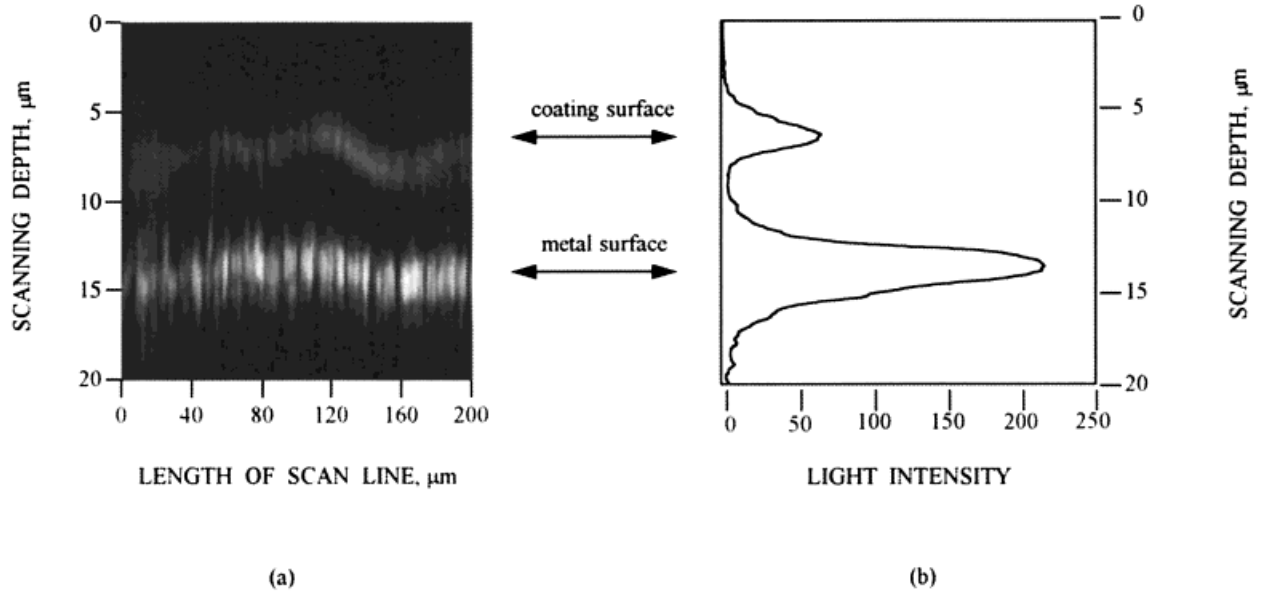

Figure 4 A maximum intensity line scan image of the sectional coating thickness profile. The line was randomly selected from the same surface as Figure 1. (a) The two bright bands highlight the top outlines of the polymer coating and metal substrate (20 × 200 μm). (b) The plot shows the variation of reflected light intensity with depth into the specimen.

the given location. The result presented in Figure 4(b) shows two peaks at depths of 6.1 and 13.3 μm (measured from a reference point), which correspond to the top points of the coating and substrate, respectively. The coating thickness at this particular location corresponds to the spacing between the peaks and is found to be 7.2 μm.

By repeating this process at a number of points along the line, the variation of thickness along the line can be determined. This allows flaws in the coating, as small as the image resolution [e.g., 0.4 μm in Fig. 4(a)], to be detected. Flaws as small as this are difficult to detect with a standard microscope.

By combining Figures 3(a) and 3(b), a volumetric portion of the polymer coating layer can be imaged, as shown in Figure 5. The density of the coating can also be estimated by combining the average coating thickness obtained above with the sample weight increase before and after electropolymerization. Thus, for a surface area of 5.5 cm^2, an average coating thickness of 7.2 μm, and a coating mass of 7.9 mg in the example shown above, a density of 1.99 g/cm^3 for the poly(2-vinylpyridine) coating is obtained. This value differs significantly from the value of 0.9985 g/cm^3 for 2-vinylpyridine monomer[52] and the value of 1.153 g/cm^3 for pure poly(2-vinylpyridine) as well.[53] However, this is not an unusual result as has been observed for a number of polymeric systems (e.g., PVC). As mentioned previously, the polymer coating is likely crosslinked and thus more compact with a higher density than the polymer formed by the bulk polymerization process. Some dense impurities may also be present in the coating.

To test this method, a coating density of 1.99 g/cm^3 was used to estimate the coating thickness for another poly(2-vinylpyridine) film produced by the same electropolymerization process after 1.5 h of cyclic potential sweep electrolysis, which had a measured mass of 5.6 mg. This yielded a thickness of 5.1 μm for this coating. This result compares favorably to a value of 5.2 μm obtained by direct graphic analysis of the light intensities from the CSLM images. This close agreement also indicates that the densities of both coatings are very similar. If the lower density of pure polymer is used, a large error is introduced in estimating the coating thickness; an even larger error is introduced when the density of the monomer is used. The results of the above sample calculation are summarized in Table I. These results suggest that coating thicknesses reported in recent publications[23] may differ considerably from the actual values.

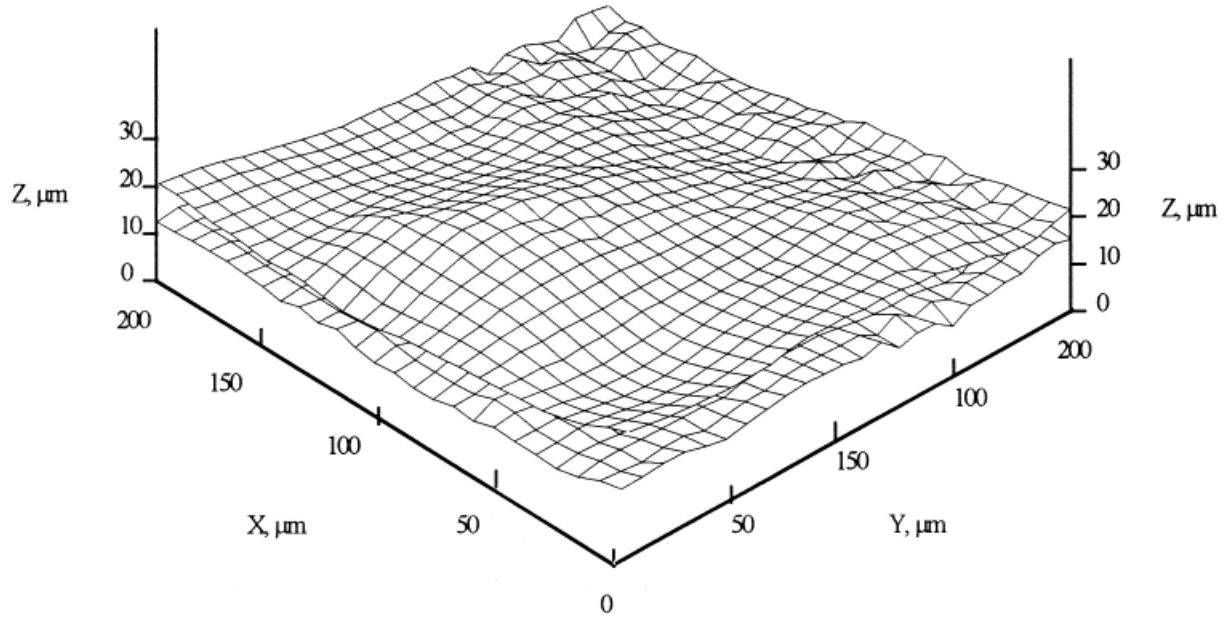

Figure 5 The volume shape of the scanned polymer coating: a combination of the images in Figures 3(a) and 3(b). The polymer coating surface is shown above the metal substrate surface.

By applying the double reflection and transmission characteristics of the modified CSLM and scanning over a relatively large surface area, it is possible to obtain information on the surface roughness distribution over the entire surface, rather than being confined to just a small area. For example, Figure 6(a) shows an image of a larger area (4×4 mm) of a poly(2-vinylpyridine) coating obtained under similar experimental conditions as mentioned previously but at a pH of 7.54. As we showed in a previous study,[13] pH has a dramatic effect on electropolymerization of poly(2-vinylpyridine). Only in a narrow pH range (4–5.5) do thick and uniform coatings form. At pH 7.54, a patchy coating forms. The irregular nature of such a coating is clearly shown in the distribution diagram of surface heights presented in Figure 6(b). The surface height gives the distance of a point on the surface to some reference point. An elevation of 0 μm corresponds to the highest surface point, while a height of 9 μm corresponds to the lowest point on the surface. It is obvious that a uniform surface should show a narrow roughness distribution, while a very irregular surface such as the one in Figure 6(a) will have a wide roughness distribution as shown in Figure 6(b). The irregular nature of the coating is further illustrated in a cross-sectioning scan (20×200 μm) in Figure 6(c). Although this scan shows that coating is present everywhere along the arbitrary direction chosen, the thickness varies from 4.5 μm at point "a" to 8 μm at point "b." It should be noted that over other portions of the substrate, no coating had formed whatsoever. Obviously, the determination of an average thickness based on the gravimetric method is meaningless for the purpose of characterizing the performance of coatings such as the one shown in Figure 6.

Table I Thickness Estimated by Different Methods

Methods	Coating Thickness (μm)
Thickness by direct measurement using CSLM	5.2
Thickness calculated from	
Coating weight (5.6 mg) and area (5.5 cm^2), using the measured polymer density of 1.99 g/cm^3	5.1
Same coating weight and area, using the pure polymer density of 1.153 g/cm^3	8.8
Same coating weight and area, using the monomer density of 0.9985 g/cm^3	10.2

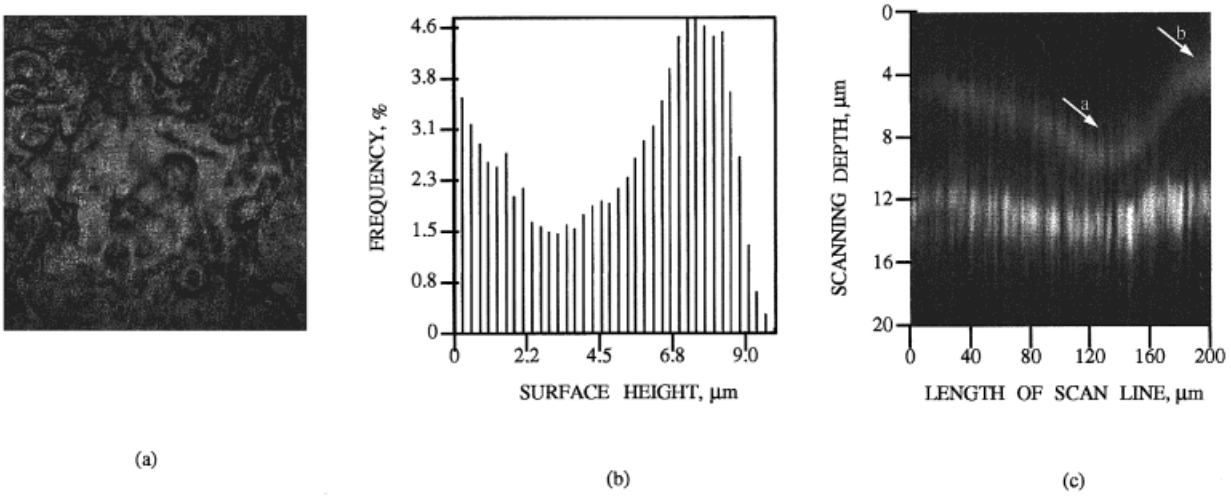

Figure 6 (a) An image (4 × 4 mm) of an irregular coating obtained with similar experimental conditions as those in Figure 1, but at a pH of 7.54. (b) Surface roughness distribution diagram of the polymer deposit in (a). Elevations of different points on the surface ranging from 0 at the top of the surface to 9 μm at the bottom of the surface, indicating an irregular surface. (c) A cross-sectioning scan of the surface along an arbitrary direction chosen (20 × 200 μm).

CONCLUSIONS

CSLM is a highly promising, nondestructive technique for analyzing the morphology of coatings. It is convenient and can accommodate large surface areas, thereby allowing the surface topography to be studied from both micro- and macroscopic points of views. High resolution images over the entire scanning surface instead of over a limited focus range can therefore be obtained. The images produced are straightforward and do not need laborious interpretation or further treatment. From the digitized images, it is easy to obtain quantitative information of the coating morphology, such as coating thickness and surface roughness distribution. The technique is particularly useful for polymer coatings that are not entirely opaque so that coating thickness and density can be readily determined. Although our application is for a poly(2-vinylpyridine) coating formed on a mild steel substrate by *in situ* electropolymerization, CSLM can be widely applied to various coating–substrate systems produced by other techniques, as long as the coatings are not completely opaque. It has proven to be a very powerful technique for analyzing the morphology of coatings.

The authors are grateful to Drs. S. Damaskinos and A. E. Dixon of the Department of Physics, University of Waterloo, for the use of the CSLM apparatus and their constructive suggestions. The authors also acknowledge financial support from the Faculty of Engineering and Department of Chemical Engineering, University of Waterloo and also from the Natural Sciences and Engineering Research Council of Canada during the course of this project.

REFERENCES

1. S. J. Sheard and M. G. Somekh, *Appl. Phys. Lett.,* **53,** 2715 (1988).
2. S. K. Yang, V. V. Varadan, and V. K. Varadan, *Mater. Eval.,* **48,** 471 (1990).
3. B. Haworth and T. M. Robinson, *Polym. Test.,* **10,** 205 (1991).
4. A. Lewis and D. Bush, *Mater. Eval.,* **49,** 132 (1991).
5. S. M. Solov'ev, *Meas. Tech.,* **34,** 1122 (1991).
6. N. V. Edneral, A. V. Ivanov, G. N. Kosyak, and E. I. Fomicheva, *Russ. J. Nondestr. Test.,* **29,** 674 (1993).
7. V. Y. Silkin and A. E. Ponomarev, *Meas. Tech.,* **36,** 997 (1993).
8. V. Roessiger and P. Raffelsberger, *Metal Finish.,* **90,** 9 (1992).
9. T. Latter, *Prod. Finish.,* **45,** 15 (1994).
10. J. Montgomery, *Mater. Eval.,* **52,** 1354 (1994).
11. F. C. Reilly, *Metal Finish.,* **92,** 49 (1994).
12. H. Hong, D. Davidov, and R. Neumann, *Adv. Mater.,* **7,** 846 (1995).
13. X. P. Ling, J. J. Byerley, M. D. Pritzker, and C. M. Burns, *J. Appl. Electrochem.,* in press.
14. G. Mengoli and B. M. Tidswell, *Polymer.,* **16,** 881 (1975).

15. F. S. Teng, R. Mahalingam, R. V. Subramanian, and R. A. V. Raff., *J. Electrochem. Soc.,* **124,** 995 (1977).
16. G. Mengoli and M. M. Musiani, *J. Electrochem. Soc.,* **134,** C643 (1987).
17. I. Sekine, K. Kohara, T. Sugiyama, and M. Yuasa, *J. Electrochem. Soc.,* **139,** 3090 (1992).
18. M. M. Musiani, F. Furlanetto, P. Guerriero, and J. Heitbaum, *J. Appl. Electrochem.,* **23,** 1069 (1993).
19. P. Denisevich, H. D. Abruna, C. R. Leidner, T. J. Meyer, and R. W. Murray, *Inorg. Chem.,* **21,** 2153 (1982).
20. R. L. McCarley, R. E. Thomas, E. A. Irene, and R. W. Murray, *J. Electrochem. Soc.,* **137,** 1485 (1990).
21. G. Mengoli, M. M. Musiani, and F. Furlanetto, *J. Electrochem. Soc.,* **137,** 162 (1990).
22. S. Taj, M. F. Ahmed, and S. Sankarapapavinasam, *J. Appl. Electrochem.,* **23,** 247 (1993).
23. A. de Bruyne, J. L. Delplancke, and R. Winand, *J. Appl. Electrochem.,* **25,** 284 (1995).
24. B. L. Funt, in *Organic Electrochemistry,* H. Lund and M. M. Baizer, Eds., Marcel Dekker, New York, 1991, p. 1337.
25. G. Mengoli, in *Advances in Polymer Science,* Vol. 33, Springer–Verlag, New York, 1979.
26. G. Mengoli and M. M. Musiani, *Electrochim. Acta,* **31,** 201 (1986).
27. G. Odian, *Principles of Polymerization,* 3rd ed., McGraw–Hill, Toronto, 1991, Chap. 4.
28. C. M. Oatley, *The Scanning Electron Microscope,* Cambridge University Press, New York, 1972.
29. J. Wang, S. P. Chen, and M. S. Lin, *J. Electroanal. Chem.,* **273,** 231 (1989).
30. H. Ohno, H. Nishihara, and K. Aramaki, *Corrosion Sci.,* **30,** 603 (1990).
31. S. Arapapavinasam, *J. Polym. Sci. Part A Polym. Chem.,* **31,** 1105 (1993).
32. S. Kunimura, T. Ohsaka, and N. Oyama, *Macromolecules,* **21,** 894 (1988).
33. T. Ohsaka, T. Hirokawa, H. Miyamoto, and N. Oyama, *Anal. Chem.,* **59,** 1758 (1987).
34. H. J. Guntherodt and R. Wiesendanger, *Scanning Tunneling Microscopy I,* Springer–Verlag, New York, 1992.
35. R. Wiesendanger and H. J. Guntherodt, *Scanning Tunneling Microscopy II,* Springer–Verlag, New York, 1992.
36. R. Wiesendanger and H. J. Guntherodt, *Scanning Tunneling Microscopy III,* Springer–Verlag, New York, 1993.
37. J. O'M. Bockris and S. U. M. Khan, *Surface Electrochemistry,* Plenum Press, New York, 1993, Chap. 1.
38. N. J. DiNardo, *Nanoscale Characterization of Surfaces and Interfaces,* VCH, Weinheim, Germany, 1994.
39. M. J. Heben, R. M. Penner, N. S. Lewis, M. M. Dovek, and C. F. Quate, *Appl. Phys. Lett.,* **54,** 1421 (1989).
40. M. P. Everson and J. H. Helms, *Synth. Metals,* **40,** 97 (1991).
41. J. P. Song, K. A. March, K. Carneiro, and A. R. Tholen, *Surface Sci.,* **296,** 299 (1993).
42. T. Ngo, L. Brandt, R. S. Eilliams, and H. D. Daesz, *Surface Sci.,* **291,** 411 (1993).
43. J. Z. Young and F. Roberts, *Nature,* **231,** 167 (1951).
44. M. Minsky, U. S. Pat. 3,013,346 (1961).
45. P. Davidovits and D. M. Egger, *Nature,* **223,** 831 (1969).
46. T. Wilson and C. Sheppard, *Theory and Practice of Scanning Optical Microscopy,* Academic Press, New York, 1984.
47. T. Wilson, *Confocal Microscopy,* Academic Press, New York, 1990.
48. A. E. Dixon, S. Damaskinos, M. R. Atkinson, and L. H. Cao, *SPIE,* **1556,** 144 (1991).
49. A. E. Dixon, S. Damaskinos, and M. R. Atkinson, *Nature,* **351,** 551 (1991).
50. X. P. Ling, Z. H. Gu, and T. Z. Fahidy, *Electrochim. Acta,* **40,** 1789 (1995).
51. P. Phillips, L. D. Freedman, and J. C. Craig, Eds., *Organic Electronic Spectral Data,* Vol. 6, Wiley–Interscience, New York, 1970, p. 110.
52. R. C. Weast and M. J. Astle, Eds., *CRC Handbook of Chemistry and Physics,* 72nd ed., CRC Press, Boca Raton, FL, 1992.
53. R. L. Miller, in *Polymer Handbook,* J. Brandrup and E. H. Immergut, Eds., 3rd ed., Wiley, New York, 1989, Chap. 6.